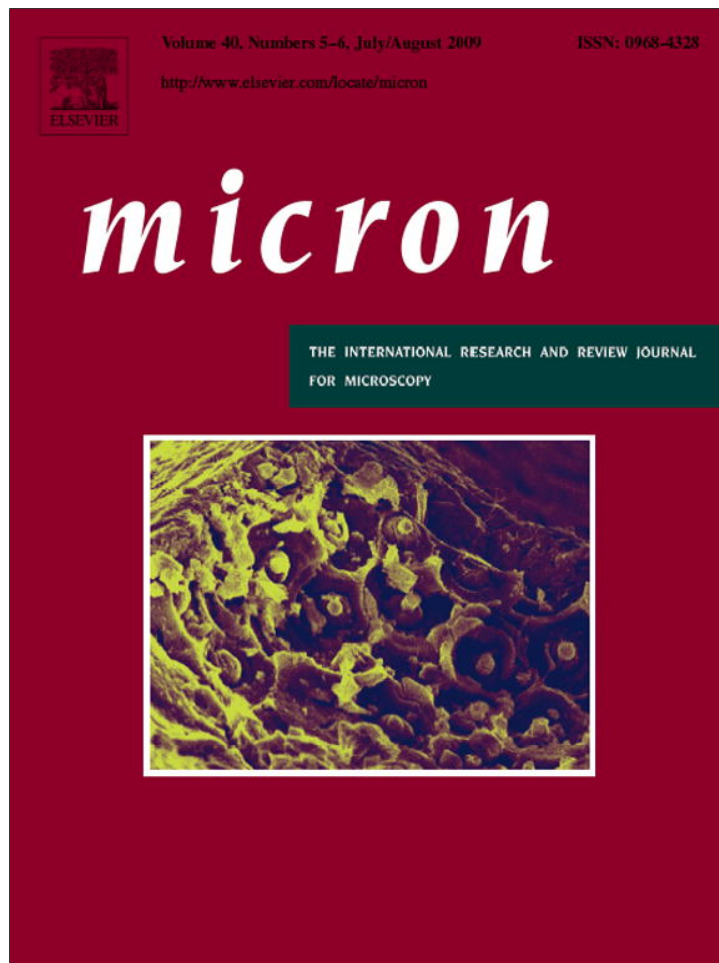


Provided for non-commercial research and education use.  
Not for reproduction, distribution or commercial use.



This article appeared in a journal published by Elsevier. The attached copy is furnished to the author for internal non-commercial research and education use, including for instruction at the authors institution and sharing with colleagues.

Other uses, including reproduction and distribution, or selling or licensing copies, or posting to personal, institutional or third party websites are prohibited.

In most cases authors are permitted to post their version of the article (e.g. in Word or Tex form) to their personal website or institutional repository. Authors requiring further information regarding Elsevier's archiving and manuscript policies are encouraged to visit:

<http://www.elsevier.com/copyright>



Contents lists available at ScienceDirect

Micron

journal homepage: [www.elsevier.com/locate/micron](http://www.elsevier.com/locate/micron)

## Evidence of multi-walled carbon nanotube fragmentation induced by sonication during nanotube encapsulation via bulk-suspension polymerization

E.A. Zaragoza-Contreras\*, E.D. Lozano-Rodríguez, M. Román-Aguirre, W. Antunez-Flores, C.A. Hernández-Escobar, Sergio G. Flores-Gallardo, A. Aguilar-Elguezabal

Centro de Investigación en Materiales Avanzados, S.C., Laboratorio Nacional de Nanotecnología, Miguel de Cervantes No. 120, C.P. 31109, Complejo Industrial Chihuahua, Chihuahua, Chih., Mexico

### ARTICLE INFO

#### Article history:

Received 17 September 2008

Received in revised form 12 February 2009

Accepted 12 February 2009

#### Keywords:

Carbon nanotubes

Nanocomposite

Suspension polymerization

Encapsulation

### ABSTRACT

The synthesis of multi-walled carbon nanotube/polystyrene composites, with nanotube concentrations of 0.04, 0.08 and 0.16 wt%, was carried out by *in situ* bulk-suspension polymerization with the assistance of sonication. By using this method both encapsulation and exfoliation of the nanotubes into the polymer host were achieved. Evidence of significant nanotube fragmentation was found by scanning electron microscopy; the cause of such fragmentation was attributed to the induction of strong cavitation due to the application of ultrasound during the synthesis. Infrared spectroscopy showed no evidence of the formation of covalent bonds between the nanotubes and the polystyrene during the process of synthesis. The thermal stability was not improved by the inclusion of the nanotubes, it was attributed to the low nanotube concentrations; however, composites glass transition temperature showed improvements.

© 2009 Elsevier Ltd. All rights reserved.

### 1. Introduction

Carbon nanotubes (CNTs) are of great interest due to their potential applications in different fields of science and technology. They offer a combination of mechanical, electrical, and thermal properties that no other material has displayed before (Coleman et al., 2006). The integration of CNT/polymer composites has been focused on the improvement of mechanical and electrical properties of the matrix (Ramanathan et al., 2005; Frankland et al., 2003; Eitan et al., 2006); however, in order to take advantages of such properties CNTs have to be both compatible and intimately dispersed within the polymer host. Nevertheless, due to strong van der Waals forces, CNTs have a great tendency to self-aggregate (Hill et al., 2002; Park et al., 2005). Several strategies have been employed to improve both compatibility and dispersion of CNTs into polymer matrixes (Sandler et al., 2003; Xie et al., 2005; Shen et al., 2005; Lee et al., 2006).

Several studies have shown that *in situ* polymerization is a reliable method for obtaining CNT/polymer composites (Funck and Kaminsky, 2007; Zhao et al., 2005), with the advantage of improving interfacial interaction to impart compatibility and to maximize CNT dispersion. In particular, the techniques of

polymerization in dispersed media have been successfully applied to encapsulate nanomaterials into polymer matrixes; with the most successful being miniemulsion polymerization, which provides proper conditions to integrate either organic or inorganic nanoparticles with the polymer matrix (Tiarks et al., 2001; López-Martinez et al., 2007; Zhang et al., 2005; Erdem et al., 2000). Nevertheless, considering the typical aspect ratios of CNTs (length/diameter) encapsulation by miniemulsion polymerization seems to be quite difficult; it would be like trying to introduce a baseball bat into a baseball ball. Reports have shown that in composites obtained via miniemulsion polymerization, the interaction between CNTs and polymer particles has been basically the adhesion of the polymer particles along the surface of the CNTs (Park et al., 2005; Vandesvorst et al., 2006; Yu et al., 2005; Ham et al., 2005). Therefore, miniemulsion polymerization or even conventional emulsion polymerization seems to be not the proper techniques to encapsulate CNTs; thus, some other options should be explored.

In this study the synthesis and the characterization of multi-walled carbon nanotube/polystyrene composites, via scanning electron microscopy and other techniques, is reported. *In situ* bulk-suspension polymerization assisted by sonication was used as the technique of synthesis, since the typical diameter of particles obtained through this technique is appropriate to perform an actual encapsulation of multi-walled carbon nanotubes (MWCNTs) into the matrix of polystyrene (PS).

\* Corresponding author. Tel.: +52 614 439 4811; fax: +52 614 439 1130.

E-mail address: [armando.zaragoza@cimav.edu.mx](mailto:armando.zaragoza@cimav.edu.mx) (E.A. Zaragoza-Contreras).

## 2. Experimental

### 2.1. Materials

MWCNTs were used without any treatment; their synthesis and characterization was reported previously (Aguilar-Elgueabal et al., 2006). Styrene monomer (Aldrich Co.) was freshly distilled under vacuum before polymerization. Nonionic surfactant OP4070 (Canamex), carboxy methyl cellulose, and sodium bicarbonate (Aldrich Co.) were used as delivered. The free radical initiator 2,2-azobisisobutyronitrile (Akzo Nobel) was recrystallized from methanol.

### 2.2. Encapsulation

MWCNT encapsulation was performed by *in situ* bulk-suspension polymerization. The procedure was the following: first, the MWCNTs (0.04, 0.08, 0.16 wt%) and the monomer (20 g) were fed to the reactor followed by application of ultrasound (2510 BRANSON ultrasonic with output of  $42 \text{ kHz} \pm 6\%$ ) for 15 min. Then the temperature was raised to  $60^\circ\text{C}$  and 2,2-azobisisobutyronitrile (0.2 g) was added in order to initiate the bulk polymerization stage. Ultrasound and mechanical agitation were applied permanently to avoid nanotube reaggregation. After 105 min of polymerization a solution of OP4070–water–carboxy methyl cellulose (80 mL), previously bubbled with nitrogen for 15 min and heated at  $70^\circ\text{C}$ , was loaded to the reactor. Sonication was maintained for 20 min longer in order to disperse the MWCNT/polystyrene molasses into the aqueous phase. The suspension polymerization stage was left to continue for 4 h in order to reach a high conversion. In all cases the polymerization's final products were millimeter-scale pearls. A blank of polystyrene was prepared, for comparison purposes, under the same conditions as the composites.

### 2.3. Characterization

MWCNT/polystyrene composites were characterized by a field emission electron microscope Jeol JSM-7401F. Before characterization, composite particle samples were washed with boiling tridistilled water in order to remove both the surfactant and colloid protector from the particle's surface. FTIR spectra of the composites were obtained using a Nicolet Magna IR Fourier Transform Spectrophotometer. Differential scanning calorimetry thermograms were run in a TA Instruments DSC Q200. Glass transition temperatures ( $T_g$ ) were taken after a process of erasing thermal memory of the sample, which consisted in heating the samples from room temperature to  $200^\circ\text{C}$ , at a heating rate of  $10^\circ\text{C}/\text{min}$  under air atmosphere; then the samples were cooled to  $40^\circ\text{C}$  and heated again to  $200^\circ\text{C}$  under the same conditions. All  $T_g$  measurements were recorded from the second heating process. Thermogravimetric analysis was carried out with a TA Instruments SDT Q600 equipment under air atmosphere and a heating rate of  $10^\circ\text{C}/\text{min}$ . Storage modulus evaluations were run in a TA Instruments RSA III, in which a temperature sweep was carried out from  $40$  to  $200^\circ\text{C}$  at fixed frequency and strain of 1 Hz and 0.1 mm respectively.

## 3. Results and discussion

### 3.1. Polymerization

During composite's synthesis two aspects were important: first, the bulk polymerization allowed an intimate dispersion of the MWCNTs into the polystyrene with the assistance of ultrasound. It is known that at high conversion bulk polymerization exhibits high viscosity and is not easy to handle. Thus the bulk polymerization

was only allowed to a conversion close to 30–35% (105 min); at times greater than 105 min (higher conversions) the viscosity was so high that the dispersion of the polymer molasses was so difficult and the polymer precipitated during suspension polymerization. Second, the polystyrene molasses (bulk polymerization) was dispersed into the aqueous phase with the aid of mechanical agitation and ultrasound; 4 h of suspension polymerization were needed to obtain solid composite particles. With decreased time (<3 h) monomer conversions were not high enough and the composite particles were still too soft and precipitation occurred.

### 3.2. Microscopy

Fig. 1 shows a SEM micrograph of the MWCNTs used in this study. They present typical diameters between 70 and 110 nm and a length of 120–140  $\mu\text{m}$  (Aguilar-Elgueabal et al., 2006), which gives an average aspect ratio (length/diameter) around 1400. Fig. 2 depicts SEM micrographs of the surface of MWCNT/PS composite particles with the three nanotube concentrations (0.04, 0.08, 0.16 wt%). As can be seen the dispersion of the MWCNTs in the surface of the composite particles was evident; it was also observed a higher density of nanotubes as the nanotube concentration increased. However, the most remarkable characteristic of these micrographs was the visible short length of the nanotubes, which was apparently below to 10  $\mu\text{m}$ . Several reports have shown such phenomenon could be due either to composite method of preparation or to nanotube chemical modification. Pötschke et al. (2004) reported that the apparently small size of MWCNTs, dispersed in polycarbonate by mechanical mixing, was a visual effect since only partial sections of individual MWCNTs were visible; i.e., parts of the nanotubes were not seen because they were inside the matrix. However, they considered it not unlikely that sample preparation had caused fractures. Gojny et al. (2006) observed a reduction of nanotube length in carbon nanotube/epoxy composites prepared by mechanical mixing. In this report, length reduction was attributed to the amino-functionalization process on the MWCNTs. Lu et al. (1996) reported that the dispersion of carbon nanotubes in a solvent, by means of ultrasound, produced a very high concentration of defects which became worse with longer periods of sonication, causing progressive nanotube degradation. Gibson et al. (2007) reported that nanotube damage was directly related to sonication time, they found that most length reduction occurred during the first 5 min of sonication. Saito et al. (2002) reported MWCNT fragmentation to lengths shorter than 1  $\mu\text{m}$  by applying sonication in mixtures of sulfuric and nitric acid.

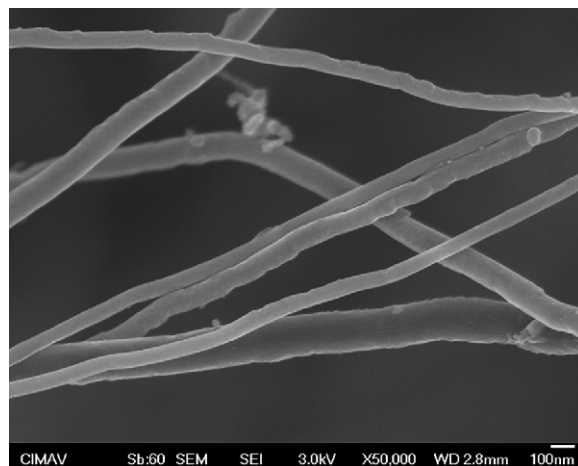
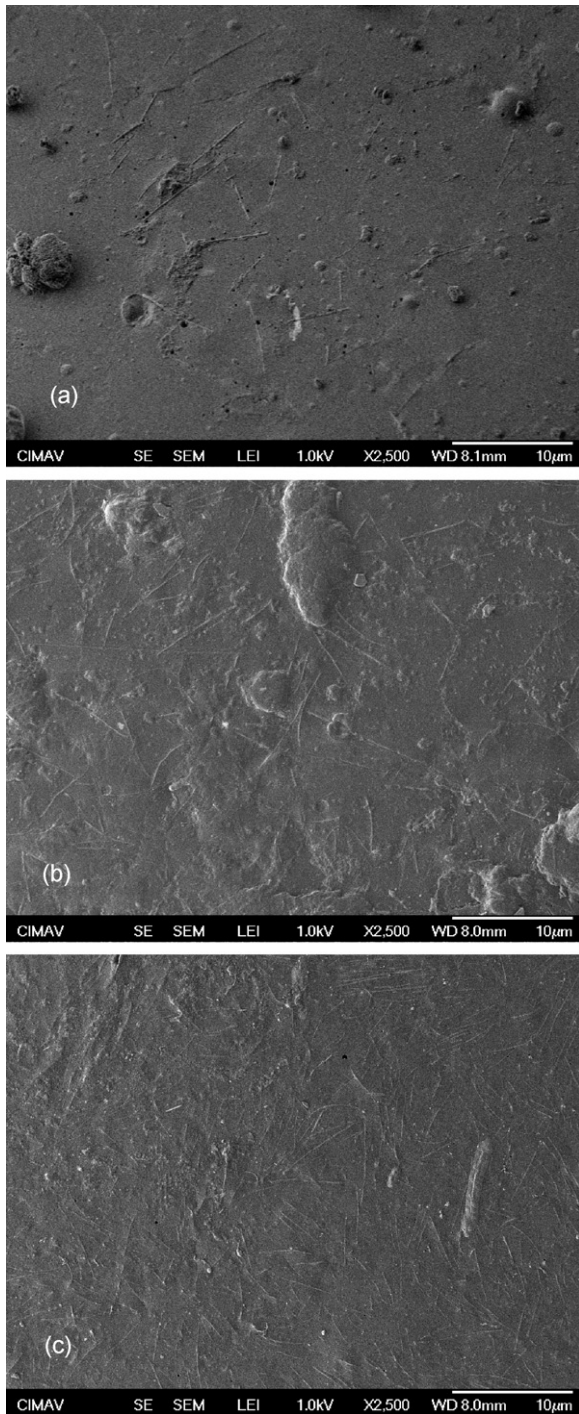
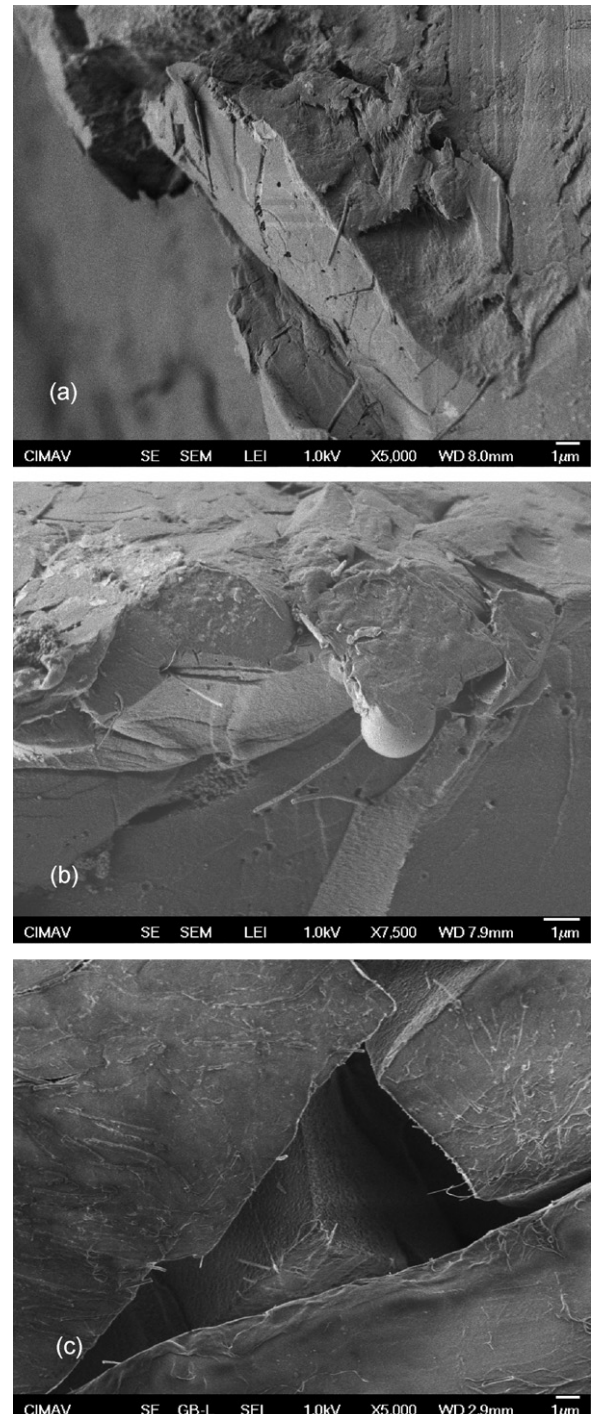


Fig. 1. Micrograph of the MWCNTs as obtained from the synthesis.



**Fig. 2.** SEM images of the MWCNTs dispersed on the surface of the composite particles: (a) 0.04 wt%, (b) 0.08 wt% and (c) 0.16 wt%.

In the present study cavitation, induced by sonication, seemed to be the cause for MWCNT fragmentation as reported by Lu et al. (1996). However, to provide a clearer vision of nanotube degradation due to cavitation or to confirm that nanotube short length was only a visual effect, due to nanotube curved structure, as suggested by Pötschke et al. (2004), composite particles with the three nanotube concentrations were fractured (frizz-fracture) and analyzed by SEM in order to observe both nanotubes distribution and nanotubes length in the bulk of the composite particles (Fig. 3(a–c)). As expected, MWCNTs were more abundantly observed with the higher concentration of nanotubes; the nanotubes were observed randomly dispersed with a more



**Fig. 3.** SEM micrographs of the freeze fracture of the MWCNT/PS composite with (a) 0.04 wt%, (b) 0.08 wt% and (c) 0.16 wt%.

abundant presence in the regions close to the surface. In respect to nanotubes length in particular in Fig. 3(c), thanks to the way as it broke, it allowed to observe much better the nanotubes in the fracture; however, MWCNT length was not enough clear to let to emit a conclusion, since one extremity (or both) of the nanotubes was sunk into the matrix. So as to obtain more solid evidence some composite particles were solved in THF and the MWCNTs observed by SEM. Fig. 4 shows a micrograph of the MWCNTs extracted as mentioned, in this case there was no doubt about nanotubes length, since they were observed complete. It was found that the nanotubes presented lengths in the range of 2–15 µm; which implicated a dramatic length reduction compared with the original

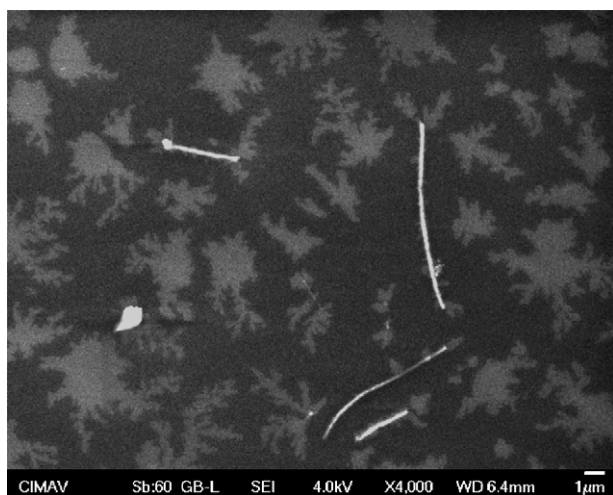


**Fig. 4.** Image of the MWCNTs obtained from the dissolution in THF of a sample of composite particles with 0.16 wt% of nanotubes.

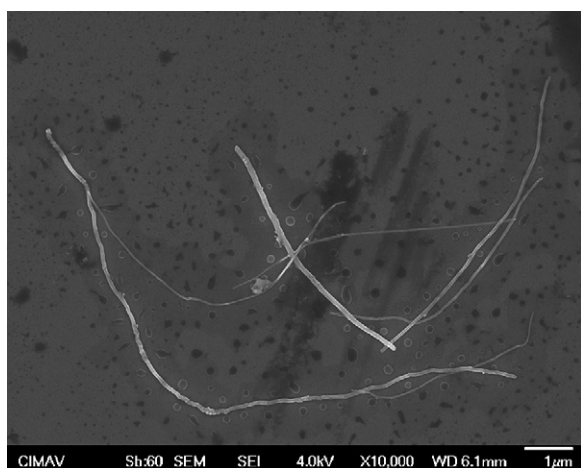


**Fig. 5.** Micrograph of pristine MWCNTs after the application of 105 min of sonication in toluene.

size (120–140 µm). Thus, MWCNT degradation took place definitely as a consequence of the process of synthesis. Additionally, a sample of pristine MWCNTs was exposed to sonication (in toluene) for 105 min at room temperature; this period was the time taken during the processes of bulk polymerization. Fig. 5 shows a SEM micrograph of the MWCNTs after sonication. As can be observed, the nanotubes also suffered from a significant length reduction; as a matter of fact the nanotubes observed in both samples (Figs. 4 and 5) show comparable dimensions. These results let us to conclude that sonication applied during bulk polymerization stage was definitely the cause for MWCNT degradation.

As a complementary remark it must be mentioned that during SEM characterization it was found evidence of the wettability of the MWCNTs with the matrix; that is, the impregnation of polystyrene onto the surface of the MWCNTs. Fig. 6 illustrates a micrograph of surface fracture of composite particles; it is clear that the nanotubes are covered by a thick layer of polystyrene. In this figure is perfectly observed that the extremities of some nanotubes are exposed, which are very thin in comparison to the rest of the body. Ding et al. (2003) reported similar observations during the preparation of nanotube–polycarbonate composites; they attributed this feature to the substantial interaction nanotube–polymer. In the present study it is believed that,

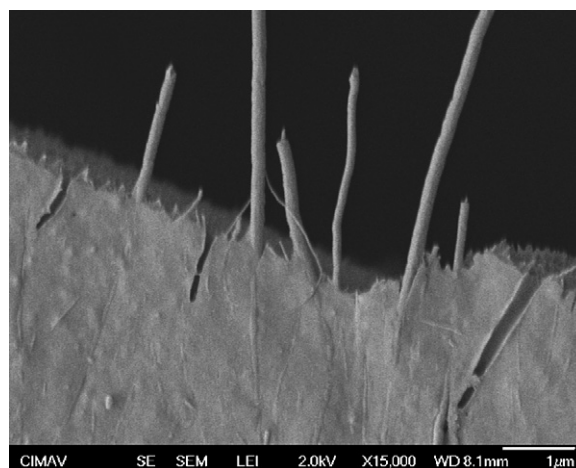


**Fig. 6.** Evidence of the wettability of the polystyrene matrix on the surface of the MWCNTs.

according to the method of synthesis, the polystyrene layer was deposited during bulk polymerization stage. The presence of such layer onto the MWCNTs surface evidences the good surface compatibility between nanotubes and polystyrene as has been reported in the literature (Hinds et al., 2004; Qian et al., 2000).

### 3.3. FTIR

Fig. 7 shows the FTIR spectrum of the MWCNT/PS composite with 0.16 wt% of nanotubes (a) and the spectrum of pure polystyrene used as the blank (b). Only one composite spectrum was presented since the three of them were identical. As can be seen both spectra presented the same signals, which corresponded to the polystyrene structure described as follows: the peaks between 3000 and 3100  $\text{cm}^{-1}$  that correspond to the bands of stretching of the group C–H of the aromatic ring; between 1600 and 2000  $\text{cm}^{-1}$  the overtones of the phenyl ring substitution; in 685 and 870  $\text{cm}^{-1}$  the bands of phenyl ring substitution; in 1602, 1500 and 1450  $\text{cm}^{-1}$  the bands of stretching of the group C=C of the aromatic ring; in 2928 and 2950  $\text{cm}^{-1}$  the bands of stretching of the groups C–H of the polymer chain. Literature indicates that in similar systems using also AIBN as the initiator and bulk or suspension polymerization, the presence of new signals has been observed. Park et al. (2005) prepared composites of poly(methyl methacrylate)/MWNT via *in situ* bulk polymerization and suspension polymerization. They found a new peak at 1650  $\text{cm}^{-1}$  which was attributed to the formation of C–C bonds between MWCNT and the poly(methyl methacrylate). Blond et al. (2006) reported

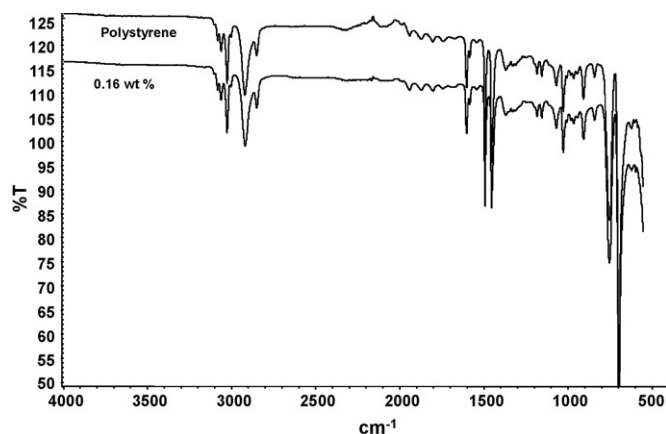


**Fig. 7.** FTIR spectra of pure polystyrene and MWCNT/PS composite with 0.16 wt%.

the grafting of poly(methyl methacrylate) onto MWCNTs. They performed the grafting by bulk polymerization using AIBN as the initiator; they observed a new peak in  $1622\text{ cm}^{-1}$  in the spectrum of FTIR of the treated MWCNTs, this signal corresponds to the C–O groups in the poly(methyl methacrylate) and represented the evidence of the grafting. Park et al. (2005) obtained MWCNT/PS composites by suspension polymerization using AIBN as the initiator. They observed two new peaks, at  $1630$  and  $991\text{ cm}^{-1}$ , in the FTIR spectrum of the composite, which increased with the increase of nanotube content. The presence of these two peaks was attributed to a C=C group and an aryl C–H bond observed in the monomer (styrene) not in the polymer, which in turn indicated that the nanotubes participated in styrene polymerization and consumed initiator. Dehonor et al. (2005) reported the grafting of polystyrene on N-doped multi-walled carbon nanotubes ( $\text{CN}_x$ ) via nitroxide mediated free radical polymerization. In this study the spectrum of FTIR of the composite PS– $\text{CN}_x$  showed no new peak(s); however, with the assistance of other characterization techniques, the authors stated that the polymer grafted covalently on the nanotubes. Wang et al. (2007) reported the grafting of polyacrylamide on single-walled carbon nanotubes via RAFT mediated free radical polymerization. They observed basically the characteristic peaks of the polyacrylamide and the RAFT agent in the spectrum of FTIR of the composite, and no new peaks; however, the analysis by Raman spectroscopy indicated the grafting reaction. In the present study no change was observed in the spectrum of FTIR of the composites, which let us to speculate first, that no reaction occurred between the polystyrene and the nanotubes even though the styrene, the MWCNTs and the AIBN were in direct contact during almost 6 h with similar conditions as in the cited literature and second, that FTIR spectroscopy, under the present conditions, does not provide the proper information to establish whether or not some reaction between the polystyrene and the nanotubes occurred.

### 3.4. Thermal analysis

In order to study the effect of the MWCNTs on the thermal properties of the MWCNT/PS composites tests of thermogravimetric analysis (TGA) and differential scanning calorimetry (DSC) were run. DSC analysis was performed in order to determine the effect of the variation of MWCNT concentration (0.04, 0.08, 0.16 wt%) on polystyrene glass transition temperature ( $T_g$ ) (Fig. 8). In this figure can be noticed that the pure polystyrene exhibits a heat flow change at approximately  $88.9^\circ\text{C}$ , corresponding to the  $T_g$  of polystyrene. On the other hand, the thermograms of the three MWCNT/PS composites displayed a small and similar increment in the  $T_g$  ( $5\text{--}6^\circ\text{C}$ ) in comparison to the pure polystyrene. The gain in  $T_g$ , even though was somewhat discrete, was attributed to a high interfacial area of interaction between the nanotubes and the matrix, which reduced the mobility of the extreme polymer chain segments. This observation could be taken as a manifestation of compatibility between the carbon nanotubes and the polystyrene matrix, which is in accordance with the literature (Hinds et al., 2004; Qian et al., 2000). It is believed that the amounts of MWCNT used in experimentation were too small to produce a more representative effect on the  $T_g$ . It is worth mentioning that reductions in  $T_g$  in carbon nanotube/polymer composites covalently grafted have been attributed to polymer low molecular weight (Shieh et al., 2005; Xu et al., 2006).

The TGA traces for the composites with the three nanotube concentrations (0.04, 0.08, 0.16 wt%) and pure polystyrene are shown in Fig. 9. As can be seen the four samples displayed a similar behaviour, with a temperature of degradation close to  $377^\circ\text{C}$ ; that is, there were no a significant effect of nanotube concentration on the composites' thermal degradation. Litera-

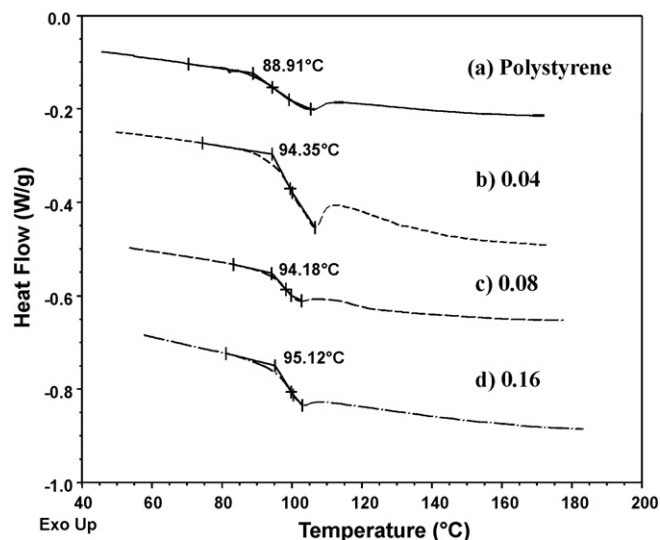


Fig. 8. DSC heating scan of (a) pure polystyrene and MWCNT/PS composites with (b) 0.04 wt%, (c) 0.08 wt% and (d) 0.16 wt%.

ture indicates increments in thermal degradation stability in nanotube/polystyrene composites in particular at nanotube concentrations higher than those used in the present study, or when the nanotubes and the polymer were bonded covalently (Costache et al., 2007; Kim et al., 2007; Zhang et al., 2006; Qin et al., 2004). From thermal characterization can be concluded that even though there was no a perceivable effect on thermal stability, due to the low nanotube concentration used, there is compatibility between the nanotubes and the polystyrene as showed by the gain in  $T_g$ .

### 3.5. DMA

The analysis of the storage modulus curves is very useful in determining the performance of a material under stress and temperature. Fig. 10 displays the dynamic mechanical spectra (storage modulus,  $\hat{E}'$ ) as function of temperature for pure polystyrene and the MWCNT/PS composites. It can be seen that the storage modulus of the MWCNT/PS composites at 0.04 and 0.08 wt% showed a minimum increment as compared to the pure

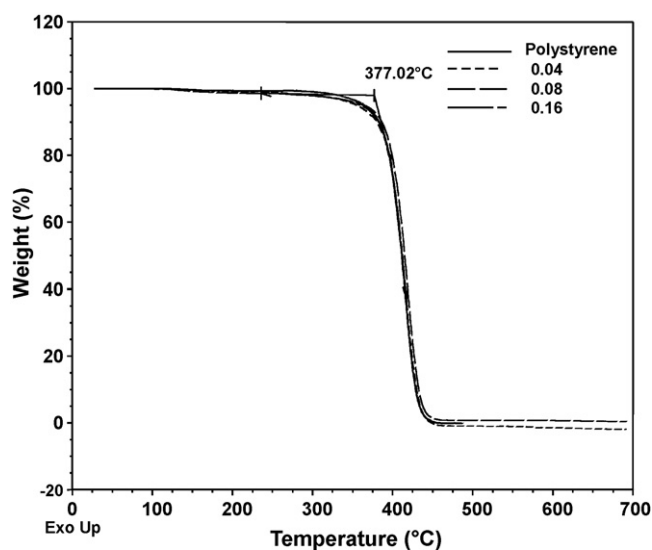


Fig. 9. TGA traces of pure polystyrene and MWCNT/PS composites with 0.04, 0.08 and 0.16 wt%. The curves are overlapped.

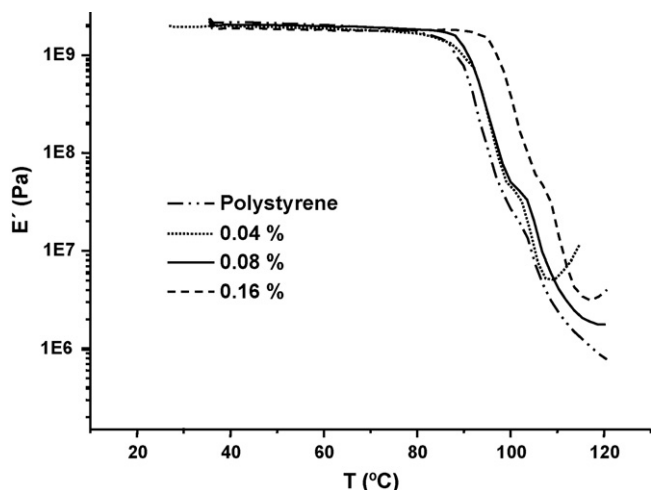


Fig. 10. DMA spectra for pure polystyrene and MWCNT/PS composites with 0.04, 0.08 and 0.16 wt%.

polystyrene; however, with the highest nanotube loading (0.16 wt%) the improvement in thermo-mechanical stability was clear, since an increment of almost 10 °C was observed. This increments, even though with the lower nanotube concentrations was small, in combination with the results of DSC and microscopy are an indication of the high compatibility between the MWCNT and the polystyrene matrix.

#### 4. Conclusions

*In situ* bulk-suspension polymerization assisted by sonication allowed the dispersion and exfoliation of the MWCNTs in the polystyrene host; however, even though sonication was an excellent way to disperse the MWCNTs into the polymer matrix, it also caused considerable nanotube degradation, which was evident by scanning electron microscopy. The characterization by infrared spectroscopy indicated no chemical reaction between the MWCNTs and the matrix, since no new peaks appeared in the spectrum. Thermogravimetric analysis showed no effect of MWCNTs on degradation temperature; however, glass transition temperature presented a small increase, which was related to high interfacial compatibility between polystyrene and the MWCNTs. This assumption was supported by DMA analysis, since increments in the storage modulus were observed, indicating the occurrence of thermo-mechanical reinforcement, which was once again related to high interfacial compatibility.

#### Acknowledgements

The authors wish to thank National Council for Science and Technology of Mexico (CONACYT) for the grant given to E.D. Lozano-Rodríguez. We wish to thank also Mónica Mendoza, Luis de la Torre, Karla Campos and Daniel Lardizaba for their helpful assistance during this research.

#### References

Aguilar-Elguezabal, A., Antunez, W., Alonso, G., Paraguay-Delgado, F., Espinosa, F., Miki-Yoshida, M., 2006. Study of carbon nanotube synthesis by spray pyrolysis and model of growth. *Diam. Relat. Mater.* 15, 1329–1335.

Blond, D., Barron, V., Ruether, M., Ryan, K.P., Nicolosi, V., Blau, W.J., Coleman, J.N., 2006. Enhanced of modulus, strength, and toughness in poly(methyl methacrylate)-based composites by the incorporation of poly(methyl methacrylate)-functionalized nanotubes. *Adv. Funct. Mater.* 16 (12), 1608–1614.

Coleman, J.N., Khan, U., Blau, W.J., Guñko, Y.K., 2006. Small but strong: a review of the mechanical properties of carbon nanotube–polymer composites. *Carbon* 44, 1624–1652.

Costache, M.C., Heidecker, M.J., Manias, E., Camino, G., Frache, A., Beyer, G., Gupta, R.K., Wilkie, C.A., 2007. The influence of carbon nanotubes, organically modified montmorillonites and layered double hydroxides on the thermal degradation and fire retardancy of polyethylene, ethylene–vinyl acetate copolymer and polystyrene. *Polymer* 48, 6532–6545.

Dehonor, M., Masenelli-Varlot, K., González-Montiel, A., Gauthier, C., Cavaillé, J.Y., Terrones, H., Terrones, M., 2005. Nanotube brushes: polystyrene grafted covalently on CN<sub>x</sub> nanotubes by nitroxide-mediated radical polymerization. *Chem. Commun.* 5349–5351.

Ding, W., Eitan, A., Fisher, F.T., Chen, X., Dikin, D.A., Andrews, R., Brinson, L.C., Schadler, L.S., Rouff, R.S., 2003. Direct observation of polymer sheathing in carbon nanotube–polycarbonate composites. *Nano Lett.* 3 (11), 1593–1597.

Eitan, A., Fisher, F.T., Andrews, R., Brinson, L.C., Schadler, L.S., 2006. Reinforcement mechanism in MWNT–filler polycarbonate. *Comp. Sci. Technol.* 66, 1162–1173.

Erdem, B., Sudol, E.D., Dimonie, V.L., El-Aasser, M.S., 2000. Encapsulation of inorganic particles via miniemulsion polymerization. *Macromol. Symp.* 155, 181–198.

Frankland, S.J.V., Harik, V.M., Odegard, G.M., Brenner, D.W., Gates, T.S., 2003. The stress–strain behavior of polymer–nanotube composite from molecular dynamics simulation. *Comp. Sci. Technol.* 63, 1655–1661.

Funck, A., Kaminsky, W., 2007. Polypropylene carbon nanotube composites by *in situ* polymerization. *Comp. Sci. Technol.* 67, 906–915.

Gibson, R.F., Ayorinde, E.O., Wen, Y.-F., 2007. Vibrations of carbon nanotubes and their composites: a review. *Comp. Sci. Technol.* 67, 1–28.

Gojny, F.H., Wichmann, M.H.G., Fiedler, B., Kinloch, I.A., Bauhofer, W., Wnidle, A.H., Schulte, K., 2006. Evaluation and identification of electrical and thermal conduction mechanisms in carbon nanotube/epoxy composites. *Polymer* 47, 2036–2045.

Ham, H.T., Choi, Y.S., Jeong, N., Chung, I.J., 2005. Singlewall carbon nanotubes covered with polypyrrole nanoparticles by the miniemulsion polymerization. *Polymer* 46, 6308–6315.

Hill, D.E., Lin, Y., Roa, A.M., Allard, L.F., Sun, Y., 2002. Functionalization of carbon nanotubes with polystyrene. *Macromolecules* 35, 9466–9471.

Hinds, B.J., Chopra, N., Rantell, T., Andrews, R., Gavalas, V., Bachas, L.G., 2004. Aligned multiwalled carbon nanotube membrane. *Science* 303, 62–65.

Kim, S.T., Choi, H.J., Hong, S.M., 2007. Bulk polymerized polystyrene in the presence of multiwalled carbon nanotubes. *Colloids Polym. Sci.* 28, 593–598.

Lee, I.S., Yoon, S.H., Jin, H.-J., Choi, H.J., 2006. Adsorption of multi-walled carbon nanotube onto poly(methyl methacrylate) microsphere and its electrorheology. *Diam. Relat. Mater.* 15, 1094–1097.

López-Martínez, E.I., Márquez-Lucero, A., Hernández-Escobar, C.A., Flores-Gallardo, S.G., Ibarra-Gómez, R., Yacamán, M.J., Zaragoza-Contreras, E.A., 2007. Incorporation of silver/carbon nanoparticles into poly(methyl methacrylate) via *in situ* miniemulsion polymerization and its influence on the glass-transition temperature. *J. Polym. Sci. Part B: Polym. Phys.* 45, 511–518.

Lu, K.L., Lago, R.M., Chen, Y.K., Green, M.L.H., Harris, P.J.F., Tsang, S.C., 1996. Mechanical damage of carbon nanotubes by ultrasound. *Carbon* 34, 814–816.

Park, S.J., Lim, S.T., Cho, M.S., Kim, H.M., Joo, J., Choi, H.J., 2005a. Electrical properties of multi-walled carbon nanotube/poly(methyl methacrylate) nanocomposite. *Curr. Appl. Phys.* 5, 302–304.

Park, J.U., Cho, S., Cho, K.S., Ahn, K.H., Lee, S.J., 2005b. Effective *in-situ* preparation and characteristics of polystyrene-grafted carbon nanotube composites. *Korea–Australia Rheol. J.* 17, 41–45.

Pötschke, P., Bhattachacharyya, A.R., Janke, A., 2004. Melt mixing of polycarbonate with multiwalled carbon nanotubes: microscopic studies on the state of dispersion. *Eur. Polym. J.* 40, 137–148.

Qian, D., Dickey, E.C., Andrews, R., Rantell, T., 2000. Load transfer and deformation mechanism in carbon nanotube–polystyrene composites. *Appl. Phys. Lett.* 76 (20), 2868–2870.

Qin, S., Qin, D., Ford, W.T., Resasco, D.E., Herrera, J.E., 2004. Functionalization of single-walled carbon nanotubes with polystyrene via grafting to and grafting from methods. *Macromolecules* 37, 752–757.

Ramanathan, P., Liu, H., Brinson, L.C., 2005. Functionalized SWNT/polymer nanocomposites for dramatic property improvement. *J. Polym. Sci. Part B: Polym. Phys.* 43, 2269.

Saito, T., Matsushige, K., Tanaka, K., 2002. Chemical treatment and modification of multi-walled carbon nanotubes. *Physica B* 323, 280–283.

Sandler, J.K.W., Kirk, J.E., Kinloch, I.A., Shaffer, M.S.P., Windle, A.H., 2003. Ultra-low electrical percolation threshold in carbon-nanotube–epoxy composites. *Polymer* 44, 5893–5899.

Shen, J., Changchun, Z., Lee, L.J., 2005. Synthesis of polystyrene–carbon nanofibers nanocomposite foams. *Polymer* 46, 5218–5224.

Shieh, Y.-T., Liu, G.-L., Hwang, K.C., Chen, C.-C., 2005. Crystallization, melting and morphology of PEO in PEO/MWCNT-g-PMMA blends. *Polymer* 46, 10945–10951.

Tiarks, F., Landfester, K., Antonietti, M., 2001. Encapsulation of carbon black by miniemulsion polymerization. *Macromol. Chem. Phys.* 202, 51–60.

Vandevorst, P., Lei, C.-H., Lin, Y., Dupont, O., Dalton, A.B., Sun, Y.-P., Keddie, J.L., 2006. The fine dispersion of functionalized carbon nanotubes in acrylic latex coatings. *Prog. Polym. Coat.* 57, 91–97.

Wang, G.-J., Huang, S.-Z., Wang, Y., Liu, L., Li, Y., 2007. Synthesis of water-soluble carbon nanotubes by RAFT polymerization. *Polymer* 48, 728–733.

Xie, X.-L., Mai, Y.-W., Zhou, X.-P., 2005. Dispersion and alignment of carbon nanotubes in polymer matrix: a review. *Mater. Sci. Eng.* 49, 89–112.

Xu, G., Wu, W.-T., Wang, Y., Pang, W., Zhu, Q., Wang, P., You, Y., 2006. Constructing polymer brushes on multiwalled carbon nanotubes by *in situ* reversible addition fragmentation chain transfer polymerization. *Polymer* 47 (16), 5909–5918.

- Yu, Y., Che, B., Si, Z., Li, L., Xue, G., 2005. Carbon nanotube/polyaniline core-shell nanowires prepared by in situ inverse microemulsion. *Synth. Met.* 150, 271–277.
- Zhang, S.-W., Zhou, S.-X., Weng, Y.-M., Wu, L.-M., 2005. Synthesis of SiO<sub>2</sub>/polystyrene nanocomposite particles via miniemulsion polymerization. *Langmuir* 21, 2124–2128.
- Zhang, Z., Zhang, J., Chen, P., Zhang, B., He, J., Hu, G.-H., 2006. Enhanced interactions between multi-walled carbon nanotubes and polystyrene induced by melt mixing. *Carbon* 44, 692–698.
- Zhao, C., Hu, G., Justice, R., Scafer, D.W., Zhang, S., Yang, M., Han, C.C., 2005. Synthesis and characterization of multi-walled carbon nanotubes reinforced polyamide 6 via in situ polymerization. *Polymer* 46, 5125–5132.